RSC Advances

PAPER

View Article Online
View Journal | View Issue

Cite this: *RSC Adv.*, 2020, **10**, 36609

A novel surface-enhanced Raman scattering method for simultaneous detection of ketamine and amphetamine

Shijiao Sun,[a] Ming Guan,*[a] Chang Guo,[b] Li Ma,[a] Hao Zhou,[d] Xiaomei Wang,[a] Fang Mi[ac] and Jiutong Li*[d]

Received 8th August 2020
Accepted 19th September 2020

DOI: 10.1039/d0ra06839j

rsc.li/rsc-advances

As common psychotropic drugs, ketamine (KET) and amphetamine (AMP) are often consumed by drug users at the same time, which seriously threatens people's health. Therefore, the study of simultaneous detection methods for KET and AMP is imperative. In this study, a novel method for the simultaneous detection of KET and AMP in serum was established on the basis of surface-enhanced Raman scattering (SERS). The antibodies were attached on Au@Ag core–shell nanoparticles embedded with different Raman reporters as the detection substrates. The labelled antigens KET–BSA and AMP–BSA were linked to carboxyl magnetic beads, and by adopting the principle of competitive immunoassay, the quantitative detections of ketamine and amphetamine were realized at the same time by detecting the Raman signals at different characteristic peaks on the magnetic beads. A good correlation was shown between ketamine and amphetamine and Raman signal response values were in the concentration range of 0–60 ng mL^{-1} and 0–200 ng mL^{-1}, and the limits of detection were 1.64 and 2.44 ng mL^{-1}. This method had the advantages of simple, rapid operation, and high sensitivity, and can realise double indicator simultaneous detection, which provided a more favorable scientific basis for preventing or reducing drug abuse, and identifying and monitoring drug users.

Introduction

In recent years, psychotropic drugs are sold extensively in recreational spots and are favored by many teenagers. The drug addiction is increasingly becoming a worldwide problem.[1] Ketamine (KET), a derivative of phenylcyclohexylpiperidine, is mainly used as a receptor antagonist of *N*-methyl-D-aspartate (NMDA). Containing the effect of anesthesia and analgesia, it can cause hallucinations by injection. It is becoming one of the favorite recreational drugs.[2] Amphetamine (AMP), is a chemical substance that can stimulate the central nervous system. It used to be the most commonly abused stimulant in sports.[3] When both are inhaled or injected in overdose, they can lead to delusion, high blood pressure and potential dyspnea. As a consequence, drug detection technology has played an important role in the prevention and control of drug abuse. It provides a scientific base for identifying the drug use, monitoring the drug treatment, and controlling after returning to society.

At present, the commonly used detection methods of ketamine and amphetamine mainly include high-performance liquid chromatography, gas chromatography, mass spectrometry,[4–7] near-infrared spectroscopy,[8] electrochemical method,[9–11] fluorescence analysis method,[12,13] the colorimetric method[14] and chemiluminescence method.[15] Although they have high sensitivity and good molecular specificity in the quantitative detection of trace drugs, their complicated sample pretreatment, time-consuming analysis procedures and high requirements on the laboratory environment still limit their applications in certain fields. In fact, most drug users are not limited to taking only one drug, and they are frequently taking two or more drugs at the same time to get more mental stimulation. The reported methods listed above can only perform quantitative detection of one drug in one injection, and it is difficult to achieve simultaneous detection of two or more drugs. Therefore, it is one of the current research hotspots to establish a method of high sensitivity, simple and fast operation, which is capable of quantitatively detecting multiple drugs at one time.

Raman spectroscopy is a kind of fingerprint spectrum which can characterize the vibration of molecular structure. Surface-enhanced Raman scattering (SERS) is an extension of Raman spectroscopy. The huge Raman scattering effect on rough surfaces of precious metal can enhance Raman signals by several orders of magnitude. It provides the possibility to

[a]*College of Chemistry and Chemical Engineering, Xinjiang Normal University, Urumqi 830054, China*
[b]*College of Pharmacy, Xinjiang Medical University, Urumqi 830011, China*
[c]*Department of Cuisine and Tourism, Bingtuan Xingxin Vocational and Technical College of Xinjiang Production and Construction Group, Urumqi 830001, China*
[d]*Shanghai Simp-Bio Science Co., Ltd, Shanghai 200000, China*

achieve the trace detection of substance molecules. In fact, the detection performance of SERS mainly depends on the enhancement ability of the substrate. Because gold and silver nanostructures can exist very stably in the air and have a surface plasmon resonance effect superior to other precious metals, they are widely used as SERS substrates for clinical test and analysis of psychotropic drugs.[16–23] Noppadon Nuntawong *et al.* used silver nanorods as a SERS substrate to detect amphetamine in urine with a detection limit of 50 ng mL^{-1}.[24] Yang *et al.* used a silver nanoneedle substrate to detect ketamine in anesthetic solution with a detection limit of 27 ng mL^{-1}.[25] Compared with single metal nanoparticles, the core–shell structured nanoparticles composed of bimetals showed stronger Raman enhancement ability as the substrate and effectively improved the sensitivity.[26,27] For example, Mao *et al.* used Au@Ag nanoparticles as a substrate to detect methamphetamine in urine, with the limit of detection as low as 0.16 ng mL^{-1}.[28] SERS technology not only has high sensitivity, simple and rapid process which does not require complicated sample pretreatment, but also can embed Raman reporters with characteristic peaks that do not interfere with each other into the Raman detection substrate to achieve multiple simultaneous quantitative detection.

In this study, a highly sensitive simultaneous detection of double indicators including ketamine and amphetamine was achieved by SERS competitive immunoassay. In the experiment, the monoclonal antibodies of ketamine and amphetamine were attached to the surface of Au-4MBA@Ag and Au-XP013@Ag nanoparticles embedded with Raman reporters 4-mercaptobenzoic acid (4MBA) and XP013, respectively. The labelled antigens KET–BSA and AMP–BSA were linked to the carboxyl magnetic beads. The labelled antigen competes with the corresponding test antigen in the sample for the monoclonal antibodies labelled on Au-4MBA@Ag and Au-XP013@Ag. The antibody labelled on Au-4MBA@Ag and Au-XP013@Ag reacts predominantly with the test antigen in the sample. The higher the concentration of the sample, the less the labelled antigen was captured by the antibody. The magnetic beads are gathered under the action of an external magnetic field, by detecting the Raman signals at the characteristic peaks of 4MBA and XP013 on the magnetic beads, the rapid and highly sensitive simultaneous detection of ketamine and amphetamine can be achieved (Fig. 1).

Materials and methods

Reagents and chemicals

Chloroauric acid, 4-mercaptobenzoic acid, ethanol, silver nitrate, trisodium citrate, ascorbic acid, 1-(3-dimethylaminopropyl)-3-ethylcarbodiimide hydrochloride, potassium chloride, sodium chloride, sodium dihydrogen phosphate dehydrate, disodium hydrogen phosphate dodecahydrate, sodium sulfide, quinol and *N*-hydroxysuccinimide were purchased from Sinopharm Group Chemical Reagent Co., Ltd. Ketamine and amphetamine standard were got from cerilliant Co., Ltd. Bovine serum albumin was obtained from Genview Co., Ltd. Calf serum was purchased from Shanghai Xiaopeng Biological Technology Co., Ltd. Carboxyl magnetic beads was got from Shanghai Taoyu International Trade Co., Ltd.

The experimental water was ultra-pure water.

Apparatus

UV spectra of Au NPs, Au-4MBA@Ag and Au-XP013@Ag were obtained by UV-vis spectrometer (L6S, Shanghai instrument Electric Scientific Instruments Co., Ltd.). Morphological characteristics of Au NPs, Au-4MBA@Ag and Au-XP013@Ag were

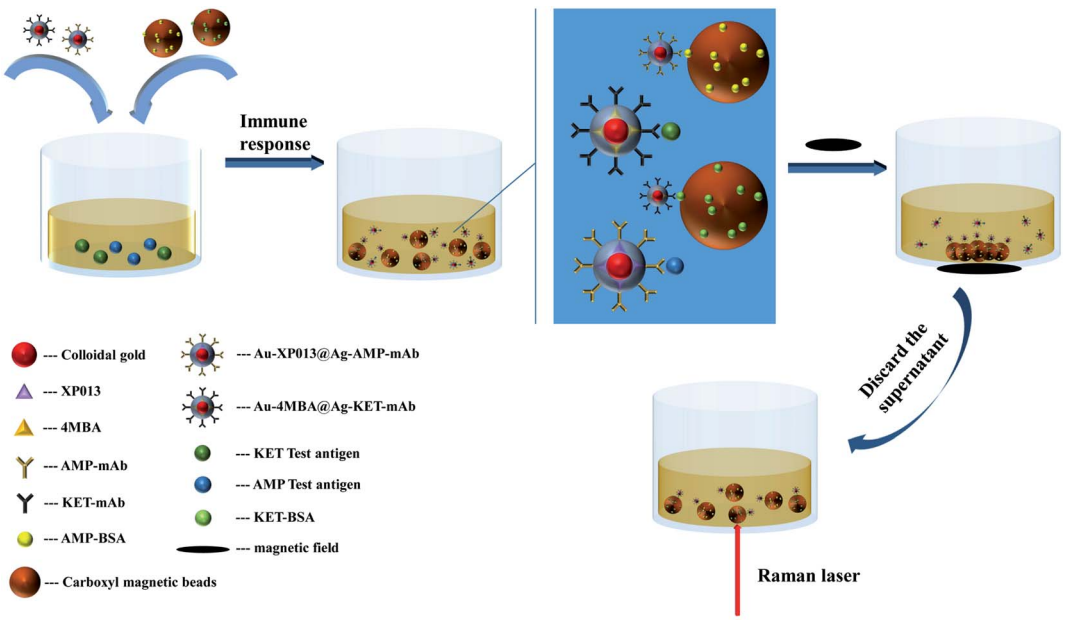

Fig. 1 Schematic representation of simultaneous detection of KET and AMP-based on SERS.

obtained by Transmission Electron Microscope (TECNAI G^2 S-TWIN). SERS spectra were obtained by Raman detector (SEED3000, Shanghai Ruhai Optoelectronics Technology Electric Co., Ltd.).

Preparation of 10 nm colloidal gold

Take 100 mL 0.01% chloroauric acid aqueous solution in the beaker, place the beaker on a magnetic agitator and heat to boiling, quickly add 5 mL 1% trisodium citrate solution, keep boiling for 30 minutes, stop heating after the solution in the beaker turns wine red, cool to room temperature, sweep the UV-visible spectrum, and the maximum absorption wavelength is about 510 nm.

Preparation of Au-4MBA@Ag and Au-XP013@Ag

Preparation of Au-4MBA@Ag. Take the colloidal gold solution of 10 nm prepared by 1 mL, add 10 μL 10 mM 4MBA, centrifuge after oscillating reaction 10 min, discard the supernatant and re-dissolves with pure water to obtain Au-4MBA. Then take 1 mL Au-4MBA and heat it to boiling, add 60 μL 20 mM $AgNO_3$ solution and trisodium citrate dropwise, trisodium citrate reduce Ag^+ to the surface of Au-4MBA, shake and mix well and place away from light until the Raman signal is no longer changed, centrifuge and remove the unreacted excess material, re-dissolve with pure water volume, and get Au-4MBA@Ag, store at 4 °C in a dark place.

Preparation of Au-XP013@Ag. Take the colloidal gold solution of 10 nm prepared by 1 mL, add 20 μL 100 mM XP013, centrifuge after oscillating reaction 10 min, discard the supernatant and re-dissolves with pure water to obtain Au-XP013. Then add 200 μL 20 mM $AgNO_3$ solution and 300 μL 0.01 M ascorbic acid solution drop by drop, reduce Ag^+ to the surface of Au-XP013 by ascorbic acid, shake and mix well and place away from light until the Raman signal is no longer changed, centrifuge and remove the unreacted excess substances, re-dissolve with pure water volume, and get Au-XP013@Ag, store at 4 °C in a dark place.

Table 1 KET and AMP series mixed standard solution concentration

Sample number	1	2	3	4	5	6
KET (ng mL^{-1})	0	5	10	20	40	60
AMP (ng mL^{-1})	0	10	20	50	100	200

Nanoparticle coupling antibody

Take the Au-4MBA@Ag and Au-XP013@Ag solutions prepared by 1 mL, add 7.5 μg KET–mAb and AMP–mAb, mix and react at room temperature for 30 minutes, then add 20 μL 10% BSA solution to react for 30 minutes, so that they occupy the remaining binding sites on the nanoparticles, centrifuge, remove unreacted excess substances, re-dissolve with 100 μL pure water, and get Au-4MBA@Ag–KET–mAb and Au-XP013@Ag–AMP–mAb, store at 4 °C.

Carboxyl magnetic bead coupling labelled antigen

Take 3 mg 3 μm carboxyl magnetic beads, add 160 μL PBS solution to mix, then add 20 μL 50 mg mL^{-1} NHS and EDC

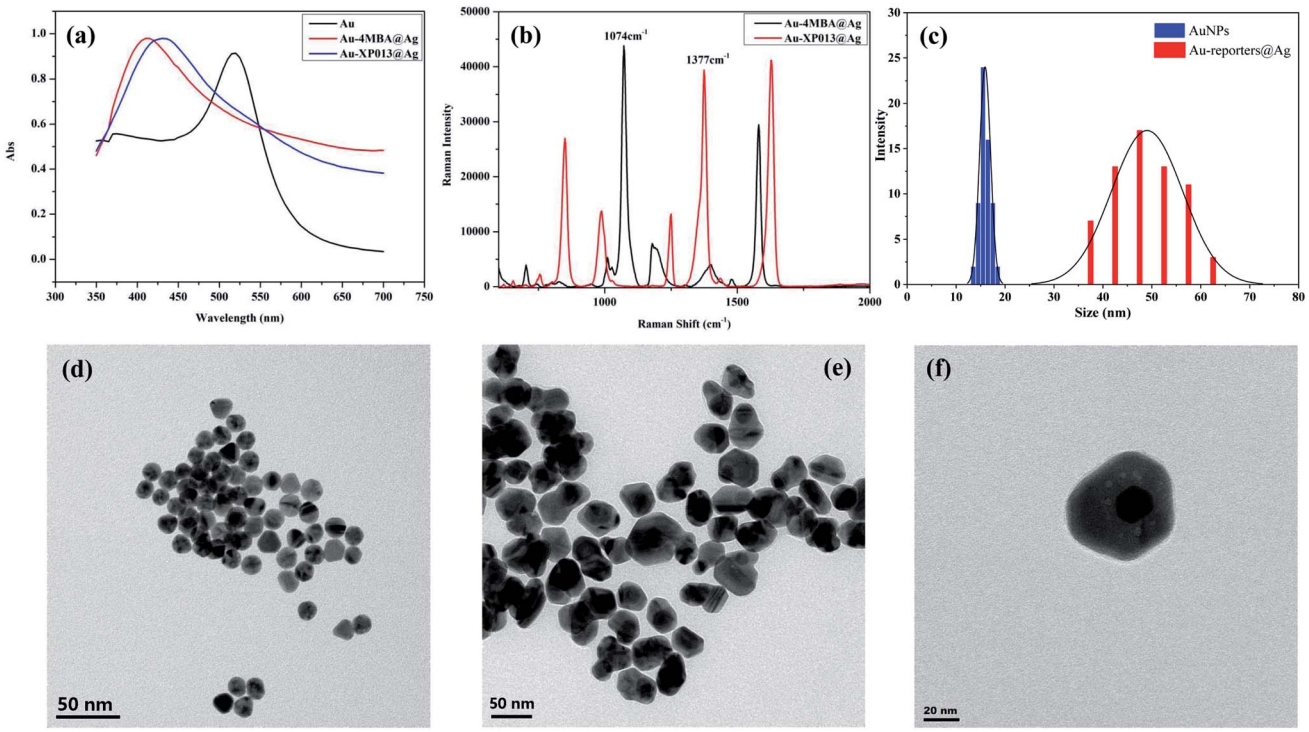

Fig. 2 UV spectra of Au NPs, Au-4MBA@Ag and Au-XP013@Ag (a), Raman spectra of Au-4MBA@Ag and Au-XP013@Ag (b), particle size distributions of Au NPs and Au-reporters@Ag (c), TEM of Au NPs (d), Au-4MBA@Ag (e) and Au-XP013@Ag (f).

Table 2 Raman signal values of KET series concentration ($n = 3$)

Concentration (ng mL^{-1})	0	5	10	20	40	60
Raman intensity	25 709 ± 871.1	16 725 ± 734.7	11 118 ± 1486	6251 ± 1057	4866 ± 666.5	2932 ± 489.9

solution, respectively, reaction away from light at 37 °C for 20 minutes, activate the carboxyl groups on the magnetic beads. Gather the magnetic beads, discard the supernatant, re-dissolve the magnetic beads in 200 μL 0.05 M MES buffer, add 2 μg labelled antigen KET–BSA and AMP–BSA, reaction at 37 °C for 2 hours, then add 20 μL 0.5 M glycine solution, stand for 15 minutes, continue to add 20 μL 10% BSA solution to react for 30 minutes, occupy the remaining binding sites on the magnetic beads, gather the magnetic beads, wash the magnetic beads with PBS solution containing 0.1% BSA twice, then add 200 μL washing solution to re-dissolve the magnetic beads. Finally, get the carboxyl magnetic beads–KET–BSA and carboxyl magnetic beads–AMP–BSA, store at 4 °C.

Preparation of a series of standard solutions

Using calf serum as the matrix solution, the KET and AMP national standard were diluted to prepare a certain concentration, and the two samples were mixed in equal volumes to make a series of mixed standard solutions (Table 1).

Results and discussion

Characterization of Au-4MBA@Ag and Au-XP013@Ag

The UV-visible absorption spectra of Au NPs, Au-4MBA@Ag, and Au-XP013@Ag in the wavelength range of 300–750 nm was listed (Fig. 2a), with the maximum absorption peak of Au at 518 nm. After Ag is coated on the surface of Au NPs, the maximum absorption peaks of Au-4MBA@Ag and Au-XP013@Ag are blue-shifted to 410 and 430 nm, which are characteristic absorption peaks of Ag, indicating the successful synthesis of Au@Ag core–shell structure. The Raman characteristic peak of Au-4MBA@Ag is at 1074 cm^{-1}, and the characteristic peak of Au-XP013@Ag is at 1377 cm^{-1}. Fig. 2b shows that the Raman characteristic peaks of Au-4MBA@Ag and Au-XP013@Ag do not interfere with each other and establish a foundation for simultaneous detection of dual indicators. Morphological characteristics of Au NPs, Au-4MBA@Ag and Au-XP013@Ag were obtained by Transmission Electron Microscope (Fig. 2d–f). We used Image J image analysis software to calculate the particle size of the nanoparticles shown in the TEM and show the histogram (Fig. 2c). The average particle size of Au NPs is 15.8 nm, and the average particle size of the nanoparticles is increased to 49.3 nm after silver coating, which proves that the thickness of the silver shell is about 33.5 nm.

Standard curve

The mixture solution (80 μL) of KET and AMP was added the mixture of Au-4MBA@Ag–KET–mAb and Au-XP013@Ag–AMP–mAb (1.5 μL each), and the mixture of carboxyl magnetic bead–KET–BSA and carboxyl magnetic bead–AMP–BSA (5 μL each). The mixture was stirred at 37 °C for 20 min. Then the magnetic beads were collected at the bottom of the reaction vessel by adding the magnetic field. The clear was discarded. After the magnetic beads were added 50 μL of PBS buffer and were fully dispersed, the Raman signal of the magnetic bead suspension was measured by Raman spectrometer. Draw the standard curve with the concentration of KET and AMP series mixed standard solution as the abscissa, the corresponding Raman signal as the ordinate (Tables 2 and 3). The regression equation for KET is $y = 11.15x^2 - 974.19x + 22\,547$, the correlation coefficient is $r = 0.9965$ (Fig. 3a); the regression equation for AMP is $y = 0.821x^2 - 250.52x + 22\,833$, the correlation coefficient is $r = 0.9998$ (Fig. 3b). The results show that KET at 0–60 ng mL^{-1} and AMP at 0–200 ng mL^{-1} have a good correlation with Raman signal. Fig. 3c shows the Raman spectra of standard curves of KET and AMP. According to the direction of the arrow, the six lines represent the Raman spectra at different concentrations of ketamine and amphetamine. It can be seen that the Raman signal is decreasing with the increase of sample concentration, which conforms to the principle of competitive immunoassay.

After 20 times of repeated determination of the blank sample, the average (M) and the standard deviation (SD) were obtained. The $M - 2$SD value was brought into the standard curve formula to get the corresponding concentration value, which was the limit of detection. The results show that when the sample concentration was 0.0 ng mL^{-1}, the limit of detection for KET was 1.64 ng mL^{-1} and the limit of detection for AMP was 2.44 ng mL^{-1}. The cut-off values specified in the ketamine and amphetamine test kits were 20 ng mL^{-1} and 25 ng mL^{-1}, respectively. The limit of detection in this study was far lower than the cut-off value, which proved that this study was competitive. By comparing the detection performances of KET and AMP in this study with other reported methods (Table 4), it is proved that this study has a good or at least comparable limit of detection and that the detection sensitivity of this study is significantly higher than other SERS methods. It is

Table 3 Raman signal values of AMP series concentration ($n = 3$)

Concentration (ng mL^{-1})	0	10	20	50	100	200
Raman intensity	25 144 ± 982.9	19 464 ± 1561	16 707 ± 229.4	11 127 ± 585.2	7615 ± 619.0	5257 ± 204.3

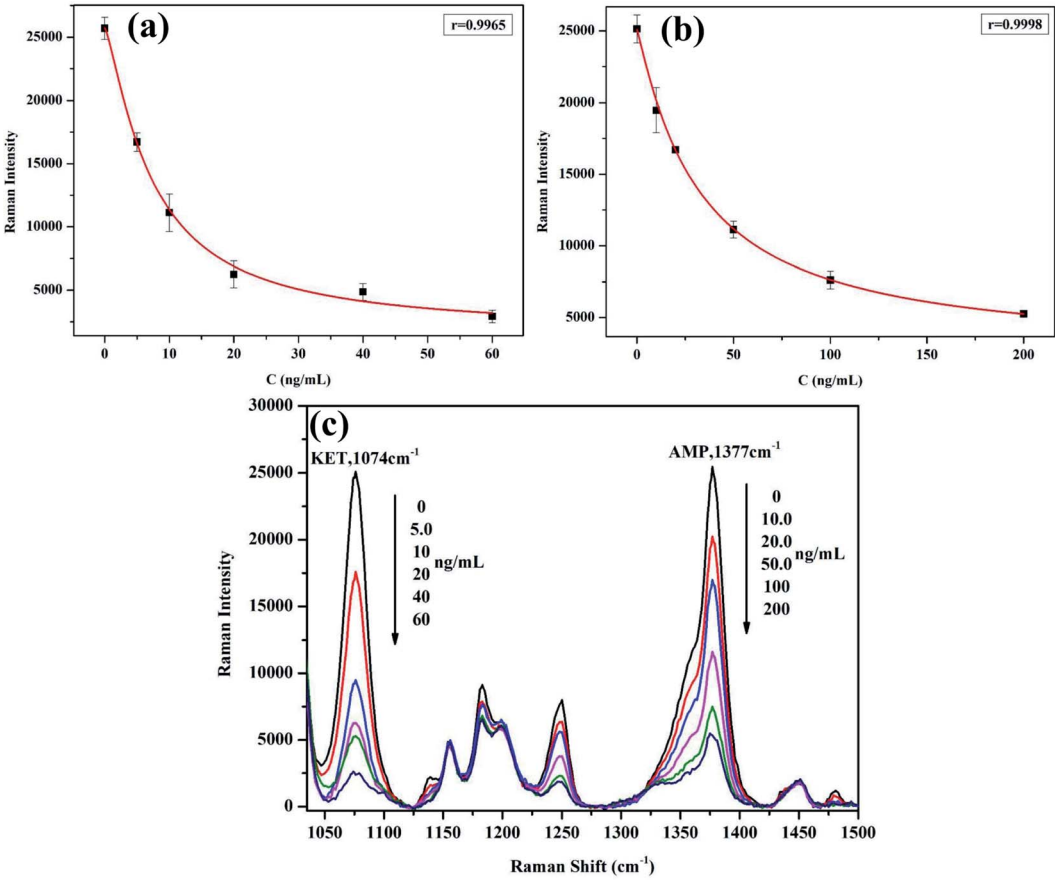

Fig. 3 Standard curve of KET (a), AMP (b), and Raman spectra of standard curves of KET and AMP (c).

Table 4 Comparison of ketamine and Amphetamine detection performances in different methods

	Methods	Sample matrix	LODs	Refs
Ketamine	LC-MS-MS	Urine	1.00 ng mL^{-1}	30
	Flurescence genosensor	Blood	0.06 ng mL^{-1}	12
	WT-ESI-MS	Urine	20.0 ng mL^{-1}	29
	SERS	Anesthetic	27 ng mL^{-1}	25
	This study	Serum	1.64 ng mL^{-1}	—
Amphetamine	GC-MS	Urine	5.00 ng mL^{-1}	4
	LC-MS-MS	Urine	5.00 ng mL^{-1}	30
	SERS	Urine	50 ng mL^{-1}	24
	This study	Serum	2.44 ng mL^{-1}	—

worth noting that the final goal of this study was the simultaneous detection of KET and AMP, while the reported methods were single-index detection.

Spike recovery experiment

Take the standard solution of 1 mL sample number 4 and add 100 μL 200 ng mL^{-1} and 5 ng mL^{-1} KET standard solution as concentration 1 and concentration 2, and then add 100 μL 200 ng mL^{-1} and 5 ng mL^{-1} AMP standard solution as concentration 3 and concentration 4, respectively. According to the above experimental steps, the Raman signal response value was

Table 5 Spike recovery experiment ($n = 3$)

	Theoretical value (ng mL^{-1})	Raman intensity	Measured value (ng mL^{-1})	Recovery rate (%)
C1	36.4	3769 ± 384.0	33.6 ± 7.5	92.4
	45.5	15 209 ± 1181	37.6 ± 6.2	82.8
C2	18.6	5656 ± 390.9	15.7 ± 1.9	84.3
	45.5	14 543 ± 861.9	40.9 ± 4.6	90.2
C3	18.2	5194 ± 654.5	18.6 ± 3.7	102.0
	63.6	11 890 ± 622.7	59.9 ± 5.9	94.2
C4	18.2	5069 ± 397.0	19.1 ± 2.8	105.1
	45.9	13 113 ± 2328	51.9 ± 15.3	113.2

Table 6 Precision experiment ($n = 10$)

	Sample number	C (ng mL^{-1})	Raman intensity	Measured value (ng mL^{-1})	CV (%)
The first batch	2	5	14 933 ± 888.9	5.4 ± 0.5	9.9
		10	23 448 ± 480.8	12.9 ± 1.9	15.0
	4	20	5562 ± 611.4	19.6 ± 2.9	14.6
		50	16 183 ± 1143	53.2 ± 8.6	16.2
	6	60	3541 ± 174.6	50.9 ± 10.4	20.4
		200	10 090 ± 725.1	159.9 ± 27.9	17.4
The second batch	2	5	17 048 ± 1401	4.7 ± 0.9	20.0
		10	19 500 ± 986.8	11.7 ± 2.4	21.2
	4	20	7712 ± 1002	17.6 ± 3.3	18.7
		50	11 383 ± 1055	49.1 ± 8.7	17.8
	6	60	3390 ± 286.1	55.3 ± 8.2	14.8
		200	5785 ± 230.2	166.5 ± 13.5	8.1
The third batch	2	5	17 538 ± 942.0	3.9 ± 0.7	19.0
		10	16 083 ± 697.3	9.0 ± 1.6	18.5
	4	20	8708 ± 352.5	17.7 ± 1.0	6.2
		50	10 194 ± 686.3	35.1 ± 5.5	15.6
	6	60	3797 ± 325.0	52.8 ± 5.4	10.2
		200	4921 ± 244.6	176.9 ± 22.3	12.6
Inter-batch	2	5	16 506 ± 1384	4.9 ± 0.8	17.0
		10	19 677 ± 3685	11.2 ± 1.9	17.7
	4	20	7327 ± 1607	18.3 ± 1.1	6.1
		50	12 586 ± 3170	45.8 ± 9.5	20.7
	6	60	3576 ± 205.8	53.0 ± 2.2	4.1
		200	6932 ± 2769	167.8 ± 8.5	5.0

obtained by Raman spectrometer, the corresponding concentration value was obtained by substituting the formula, and the recovery rate was calculated (Table 5). The results show that the recoveries of the four concentration points are all in the range of 80–115%, indicating that the detection method is accurate and can be used for the simultaneous detection of KET and AMP.

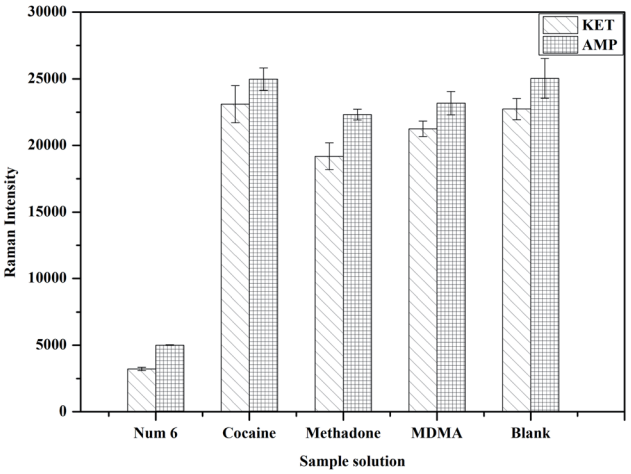

Fig. 4 Specificity experiment ($n = 3$).

Precision experiment

Three batches of SERS tags were prepared, according to the above experimental steps, the low, medium and high concentration points of sample numbers 2, 4 and 6 were detected respectively. The Raman signal response value was obtained by Raman spectrometer, and the corresponding concentration value was obtained, the average value of Raman signal and its corresponding concentration (M) and standard deviation (SD),

Table 7 Interfering experiment ($n = 3$)

Interfering substances	Sample number	C (ng mL^{-1})	Raman intensity	Measured value (ng mL^{-1})	Recovery rate (%)
Bilirubin	2	5	17 193 ± 965.9	4.2 ± 0.8	85.9
		10	26 595 ± 1473	9.4 ± 4.3	94.1
	4	20	9196 ± 889.8	16.5 ± 2.7	82.8
		50	17 011 ± 647.2	50.5 ± 4.8	101.1
	6	60	4557 ± 598.6	58.8 ± 14.7	98.0
		200	8339 ± 588.1	176.0 ± 15.2	88.0
EDTA	2	5	16 307 ± 711.0	5.0 ± 0.6	100.8
		10	25 670 ± 1202	10.1 ± 3.3	101.2
	4	20	8050 ± 1194	21.0 ± 4.8	105.1
		50	16 137 ± 434.1	57.3 ± 3.5	114.8
	6	60	4870 ± 876.0	52.9 ± 17.0	88.1
		200	8049 ± 614.9	184.0 ± 16.6	92.0
Trisodium citrate	2	5	15 469 ± 979.9	5.8 ± 0.9	116.9
		10	24 985 ± 383.7	11.9 ± 1.1	119.0
	4	20	8883 ± 154.1	17.3 ± 0.4	86.6
		50	16 135 ± 793.6	57.5 ± 6.4	115.0
	6	60	4828 ± 307.6	50.3 ± 5.9	83.9
		200	8593 ± 626.1	169.5 ± 16.0	84.7
Hemoglobin	2	5	15 321 ± 1193	6.0 ± 1.1	120.3
		10	25 156 ± 1009	11.5 ± 2.8	115.1
	4	20	7603 ± 722.2	24.0 ± 4.4	120.0
		50	15 929 ± 756.6	59.2 ± 6.6	118.5
	6	60	4533 ± 331.1	64.3 ± 8.4	107.3
		200	8641 ± 301.7	167.8 ± 7.6	83.9

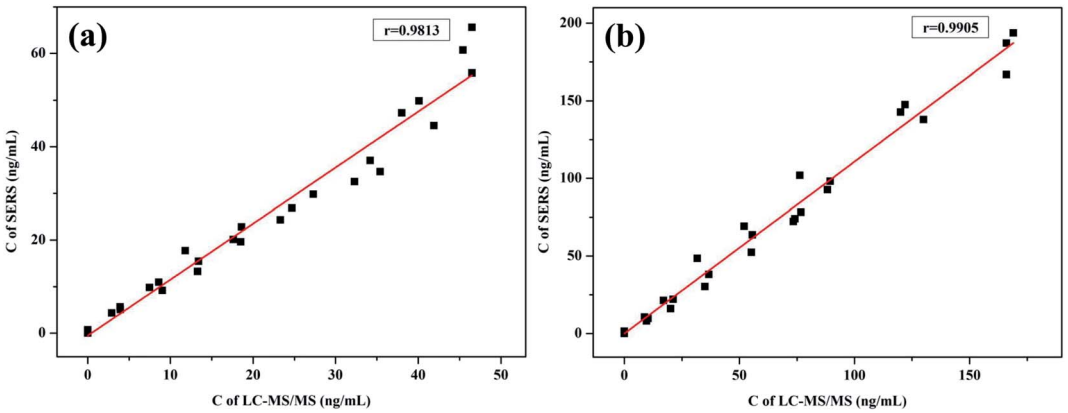

Fig. 5 Comparison of SERS and LC-MS/MS method for the simultaneous detection of KET (a) and AMP (b).

were calculated according to the formula coefficient of variation (CV) = SD/M × 100%, and the concentration CV, of each concentration point was obtained (Table 6). The results showed that three batches of SERS tags were used for the simultaneous detection of KET and AMP at low, medium and high concentration points, the concentration CV was about 15%, and the precision was relatively good.

Interfering experiment

Take 1 mL low, medium and high concentration points of samples numbered 2, 4 and 6, add 20 μL of common interfering substances in serum, bilirubin, hemoglobin, and common anticoagulants in blood, ethylenediaminetetraacetic acid (EDTA), trisodium citrate, respectively. The final concentrations of the four substances were 2 mg mL^{-1}, 10 mg mL^{-1}, 1.5 mg mL^{-1} and 0.1 mg mL^{-1}. According to the above experimental steps, the Raman response signal value was measured by Raman spectrometer, the corresponding concentration value was obtained by substituting the formula, and the recovery rate was calculated (Table 7). The result shows that when the sample contains four interfering substances: bilirubin, hemoglobin, EDTA and trisodium citrate, the recoveries of low, medium and high concentrations are basically between 85% and 115%, indicating that the four interferers will not interfere with the detection results.

Specificity experiment

Select the high concentration point with sample number 6 as a control, and take the high concentration cocaine, methadone and ecstasy with a sample concentration of 1000 ng mL^{-1} as interferences. According to the above experimental steps, the Raman response signal values were obtained by Raman spectrometer. The results show that high concentration of cocaine, methadone and MDMA interferers and blank samples all produced strong Raman signals, while sample 6 only produced weak Raman signals (Fig. 4), indicating that this method has good specificity in the simultaneous detection of KET and AMP.

Comparative experiment

Simultaneous detection of 27 KET and AMP mixed standard samples by SERS and LC-MS/MS, the quantitative detection results of the two methods were subjected to T-test and using SPSS 22.0 statistical software-related analysis. The results show that the KET T-test results $t = -0.768$, $p = 0.446 > 0.05$, indicating that the results measured by the two methods have no statistical difference, the linear regression equation $y = 0.802x + 1.1793$, the correlation coefficient $r = 0.9813$, indicating that the two methods have a good correlation (Fig. 5a). The AMP T-test results $t = -0.436$, $p = 0.665 > 0.05$, indicating that the results measured by the two methods have no statistical difference, the linear regression equation $y = 0.8863x + 1.2142$, the correlation coefficient $r = 0.9905$, indicating that the two methods have a good correlation (Fig. 5b).

Conclusion

In this study, surface-enhanced Raman scattering (SERS) was used to establish a rapid and highly sensitive method for the simultaneous detection of ketamine and amphetamine in serum, on the basis of the principle of competitive immunoassay. In the experiment, monoclonal antibodies with KET and AMP were labelled on Au@Ag embedded with different Raman reporters, and KET and AMP labelled antigens were directly connected on carboxyl magnetic beads. After the immune response, the Raman signals at different characteristic peaks on magnetic beads were detected to achieve simultaneous detection of KET and AMP in serum. The limits of detection were 1.64 and 2.44 ng mL^{-1}, respectively. Compared with the reported gas, liquid chromatography, fluorescence analysis method and other detection methods, SERS does not need complex sample pretreatment procedures and has the advantages of simple, rapid detection process, high sensitivity and low technical requirements for laboratory environment and testing personnel. In addition, the Raman spectrometer has gradually developed to the portable direction, which is easier to meet the needs of convenient and rapid detection of drugs.

Conflicts of interest

There are no conflicts to declare.

Acknowledgements

This work is supported by the National Natural Science Foundation of China (22064016), Natural Science Foundation of Xinjiang Uygur Autonomous Region (2019D01A69, 2019D01B36), Xinjiang Uygur Autonomous Region University Scientific Research Program Key Project (XJEDU2019I019), the Scientific Research and Development Project of Xinjiang normal University (XJNUZX202003), the Doctoral Research and Innovation Program of Xinjiang normal University (XJ107622007), Xinjiang Uygur Autonomous Region University Scientific Research Program Youth Project (XJEDU2018Y030) and Outstanding Young Science and Technology Talents Project of Tianshan Youth Plan in Xinjiang Uygur Autonomous Region (2017Q027).

References

1 A. L. Castro, S. Tarelho, A. J. Silvestre and H. M. Teixeira, *J. Forensic Leg. Med*, 2012, **19**, 77–82.
2 C. J. A. Morgan and H. V. Curran, *Addiction*, 2011, **107**, 27–38.
3 M. Martens, H. Zurhold, M. Rosenkranz, A. Odonnell, M. Addision, L. Spencer, W. Mcgovern, R. Gabrhelik, B. Petruzelka, M. Rowicka, N. Liebregts, P. Degkwitz, E. Kaner and U. Verthein, *Harm Reduct. J.*, 2020, **17**, 36–42.
4 K. A. Alsenedi and C. Morrison, *Anal. Methods*, 2018, **10**, 1431–1440.
5 K. M. Clauwaert, J. F. Van Bocxlaer, E. A. De Letter, S. Van Calenbergh, W. E. Lambert and A. P. De Leenheer, *Clin. Chem.*, 2000, **46**, 1968–1977.
6 H. Khajuria and B. P. Nayak, *Egypt. J. Forensic Sci.*, 2016, **6**, 337–341.
7 E. Gerace, D. Canepar, F. Borio, A. Salomone and M. Vincenti, *J. Separ. Sci.*, 2019, **42**, 1577–1584.
8 R. M. Correia, E. Domingos, F. Tosato, N. A. Dos Santos, J. De ALeite, M. DaSilva, M. C. A. Marcelo, R. S. Ortiz, P. R. Filgueiras, W. Romao and F. Tosato, *Anal. Methods*, 2018, **10**, 593–603.
9 H. J. Li, X. J. Hu, J. L. Zhao, K. Koh and H. X. Chen, *Electrochem. Commun.*, 2019, **100**, 126–133.
10 Y. Chen, Y. Yang and Y. F. Tu, *Sensor. Actuator.*, 2013, **183**, 150–156.
11 Y. Yang, S. Y. Zhai, C. Liu, X. S. Wang and Y. F. Tu, *Acs Omega*, 2019, **4**, 801–809.
12 Y. J. Ding, X. G. Li, Y. D. Guo, J. Yan, J. Ling, W. C. Li, L. M. Lan, Y. F. Chang, J. F. Cai and L. Zha, *Anal. Bioanal. Chem.*, 2017, **409**, 7027–7034.
13 H. Chen, Y. Zou, X. Jiang, F. Q. Cao and W. B. Liu, *RSC Adv.*, 2019, **9**, 36884–36889.
14 B. Maddah, V. Alimardani and H. Moradifard, *Anal. Methods*, 2015, **7**, 10364–10370.
15 C. X. Li, Y. H. Yang and D. S. Leng, *J. Liaoning Univ. Tradit. Chin. Med.*, 2019, **21**, 192–196.
16 G. S. Bumbrah and R. M. Sharma, *Egypt. J. Forensic Sci.*, 2016, **6**, 209–215.
17 X. N. Yan, P. Li, B. B. Zhou, X. H. Tang, X. Y. Li, S. Z. Weng, L. B. Yang and J. H. Liu, *Anal. Chem.*, 2017, **89**, 4875–4881.
18 F. Inscore, C. Shende, A. Sengupta, H. Huang and S. Farquharson, *Appl. Spectrosc.*, 2011, **65**, 1004–1006.
19 V. Delia, G. M. Garcia and C. G. Ruiz, *Appl. Spectrosc. Rev.*, 2015, **50**, 775–796.
20 E. L. Izake, *Forensic Sci. Int.*, 2010, **202**, 1–8.
21 T. X. Yang, X. Y. Guo, H. Wang, S. Y. Fu, Y. Wen and H. F. Yang, *Biosens. Bioelectron.*, 2015, **68**, 350–357.
22 C. A. Penido, M. T. Pacheco, I. K. Lednev and L. Silveira, *J. Raman Spectrosc.*, 2016, **47**, 28–38.
23 Y. Q. Wang, B. Yan and L. X. Chen, *Chem. Rev.*, 2013, **113**, 1391–1428.
24 N. Nuntawong, P. Eiamchai, W. Somrang, S. Denchitcharoen, S. Limwichean, M. Horprathum, V. Patthanasettakul, S. Chaiya, A. Leelapojanaporn, S. Saiseng, P. Pongsethasant and P. Chindaudom, *Sensor. Actuator. B Chem.*, 2017, **239**, 139–146.
25 Y. Yang, Z. Y. Li, K. Yamaguchi, M. Tanemura, Z. R. Huang, D. L. Jiang, Y. H. Chen, F. Zhou and M. Nogami, *Nanoscale*, 2012, **4**, 2663–2669.
26 K. Q. Wang, D. W. Sun, H. B. Pu and Q. Y. Wei, *Talanta*, 2019, **191**, 449–456.
27 B. B. Nie, Y. Y. Luo, J. P. Shi, L. Gao and G. T. Duan, *Sensor. Actuator. B Chem.*, 2019, **301**, 127087.
28 K. Mao, Z. L. Zhou, S. Han, X. D. Zhou, J. M. Hu, X. Q. Li and Z. G. Yang, *Talanta*, 2018, **190**, 263–268.
29 P. So, T. Ng, H. X. Wang, B. Hu and Z. P. Yao, *Analyst*, 2013, **138**, 2239–2243.
30 C. Yang, H. C. Liu, D. L. Lin, R. H. Liu, Y. Z. Hsieh and S. P. Wu, *J. Anal. Toxicol.*, 2017, **41**, 679–687.

